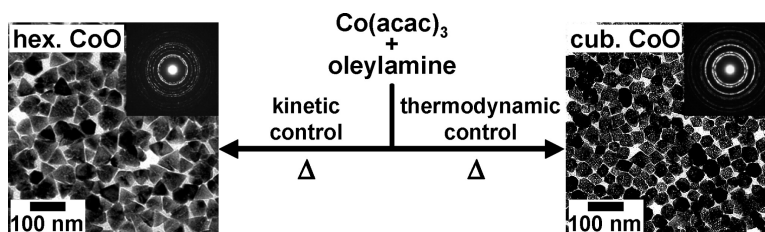


## Phase- and Size-Controlled Synthesis of Hexagonal and Cubic CoO Nanocrystals

Won Seok Seo, Jae Ha Shim, Sang Jun Oh, Eun Kwang Lee, Nam Hwi Hur, and Joon T. Park

*J. Am. Chem. Soc.*, **2005**, 127 (17), 6188-6189 • DOI: 10.1021/ja050359t • Publication Date (Web): 09 April 2005

Downloaded from <http://pubs.acs.org> on March 25, 2009



### More About This Article

Additional resources and features associated with this article are available within the HTML version:

- Supporting Information
- Links to the 29 articles that cite this article, as of the time of this article download
- Access to high resolution figures
- Links to articles and content related to this article
- Copyright permission to reproduce figures and/or text from this article

[View the Full Text HTML](#)

## Phase- and Size-Controlled Synthesis of Hexagonal and Cubic CoO Nanocrystals

Won Seok Seo,<sup>†</sup> Jae Ha Shim,<sup>†</sup> Sang Jun Oh,<sup>‡</sup> Eun Kwang Lee,<sup>§</sup> Nam Hwi Hur,<sup>\*,§</sup> and Joon T. Park<sup>\*,†</sup>

National Research Laboratory, Department of Chemistry and School of Molecular Science (BK 21), Korea Advanced Institute of Science and Technology, Daejeon, 305-701, Korea, Korea Basic Science Institute, Daejeon, 305-333, Korea, and Center for CMR Materials, Korea Research Institute of Standards and Science, Daejeon, 305-600, Korea

Received January 19, 2005; E-mail: joontpark@kaist.ac.kr; nhhur@kriss.re.kr

Transition metal oxide nanocrystals have a wide range of applications in magnetic data storage, battery materials, catalysts, sensors, and ferrofluids, mainly due to their chemical stability and magnetic properties.<sup>1</sup> Developing new methods for the preparation of metal oxide nanocrystals with various sizes and shapes and investigating their properties are thus of considerable interest.<sup>2</sup> In particular, cobalt monoxide (CoO) nanocrystals are significant owing to their potential applications based on magnetic, catalytic, and gas-sensing properties.<sup>3</sup> Thus far, however, few methods have been reported for the synthesis of CoO nanocrystals exclusively with a cubic rock-salt structure.<sup>4</sup>

Herein we report results of a reliable synthesis of CoO nanocrystals using a single precursor, Co(acac)<sub>3</sub> (acac = acetylacetonate). Remarkably, new wurtzite-type hexagonal CoO nanocrystals never observed in bulk CoO have been isolated along with the well-known cubic phase. ZnO is the only stable metal oxide previously discovered to possess such a hexagonal structure.

Typical synthetic procedures are as follows.<sup>5</sup> A green slurry of cobalt precursor Co(acac)<sub>3</sub> in oleylamine was heated at 135 °C under an Ar atmosphere. Immediately after dissolution, the reaction was initiated by flash-heating to 200 °C. After being annealed for 1 h, the reaction mixture was cooled to room temperature, giving green hexagonal CoO nanocrystals separated by centrifugation and purified by washing with ethanol. Cubic CoO nanocrystals were synthesized under similar synthetic conditions using longer reaction time at 135 °C. The green reaction mixture was heated at 135 °C for 5 h under an Ar atmosphere, which slowly became red. This solution was flash-heated to 200 °C and annealed for 3 h, giving brown cubic CoO nanocrystals obtained by a similar workup procedure.

EDX spectrometry and EELS<sup>5</sup> for both nanocrystals yielded an average atomic ratio of 49:51 (Co/O), which can be considered to have almost stoichiometric compositions. The XRD patterns of the CoO samples provided in Figure 1 clearly show pure nanocrystalline hexagonal and cubic phases. The diffraction peaks of the cubic phase (Figure 1d–f) are well matched with those of the corresponding bulk CoO congener (*Fm*3*m*, *a* = 4.26 Å), while peaks are slightly broadened with decreasing nanocrystal size. As given in Figure 1a–c, the diffraction patterns from hexagonal CoO nanocrystals are in good agreement with those from hexagonal ZnO (*P*6<sub>3</sub>*mc*, *a* = 3.25 Å and *c* = 5.21 Å). The calculated lattice parameters of *a* and *c* are 3.2518(2) and 5.1967(3) Å, respectively, which is quite close to those of ZnO.

The low- and high-resolution TEM images of various hexagonal CoO nanocrystals are illustrated in Figure 2. When a solution of 1:200 molar ratio of Co(acac)<sub>3</sub> and oleylamine was employed, rod-

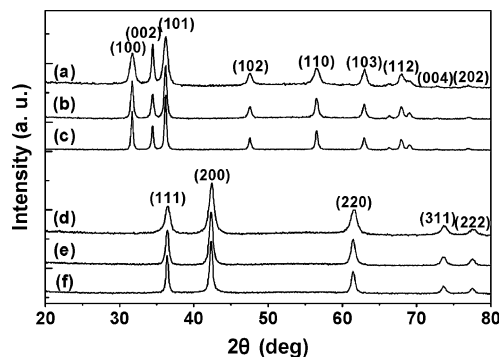


**Figure 1.** XRD patterns of (a) 11 × 40 nm rod-shaped and (b) 47 nm and (c) 83 nm hexagonal pyramid-shaped hexagonal CoO nanocrystals. XRD patterns of (d) 13 nm, (e) 24 nm, and (f) 33 nm cubic CoO nanocrystals.

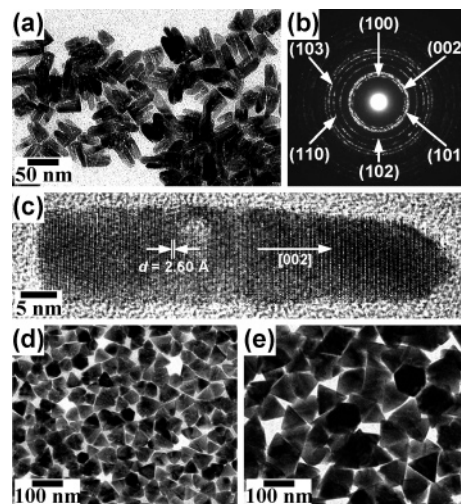


**Figure 2.** TEM micrographs of hexagonal CoO nanocrystals: (a) TEM image, (b) SAED pattern, and (c) HRTEM image of rod-shaped nanocrystals with average width of 11 ± 1.7 nm and average length of 40 ± 7.3 nm. TEM images of hexagonal pyramid-shaped nanocrystals with average side edge lengths of (d) 47 ± 4.6 nm and (e) 83 ± 9.2 nm.

shaped CoO nanocrystals were formed. Figure 2a shows rod-shaped nanocrystals with 11 ± 1.7 nm in width and 40 ± 7.3 nm in length. The strong ring patterns from SAED given in Figure 2b can be well indexed to the wurtzite structure. This is consistent with the XRD data given in spectra a–c of Figure 1. The HRTEM image in Figure 2c reveals that nanorods are grown along the unique *c* axis of the hexagonal structure, which coincides with narrow (002) peak in XRD of Figure 1a.<sup>6</sup> The observed lattice spacing corresponding to the (002) lattice plane is estimated to be 2.60 Å. Interestingly, size and shape of the CoO nanocrystals can be controlled by changing the precursor concentration. For example, hexagonal pyramid-shaped CoO nanocrystals of 47 ± 4.6 nm in

<sup>†</sup> Korea Advanced Institute of Science and Technology.

<sup>‡</sup> Korea Basic Science Institute.

<sup>§</sup> Korea Research Institute of Standards and Science.

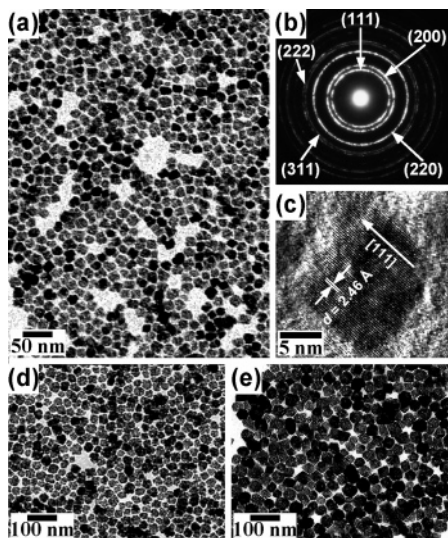


**Figure 3.** TEM micrographs of cubic CoO nanocrystals: (a) TEM image, (b) SAED pattern, and (c) HRTEM image of  $13 \pm 1.6$  nm nanocrystals. TEM images of (d)  $24 \pm 3.3$  nm and (e)  $33 \pm 4.5$  nm nanocrystals.

side edge length and  $24 \pm 2.4$  nm in basal edge length (Figure 2d) were obtained when a solution of 1:100 molar ratio of  $\text{Co}(\text{acac})_3$  and oleylamine was used. Similar shaped but larger nanocrystals of  $83 \pm 9.2$  nm in side edge length and  $42 \pm 4.5$  nm in basal edge length (Figure 1e) were grown from a 1:50 molar ratio solution. The hexagonal pyramidal shape was confirmed by tilting the hexagon or triangle TEM images, in which the basal plane of the hexagonal pyramid is (002) and the direction from the base to the top of the hexagonal pyramid is [002].<sup>5</sup> Apparently hexagonal pyramid-shaped nanocrystals are predominant over nanorods in bigger nanocrystals, which are favored by abrupt decomposition in higher precursor concentration.

Figure 3 shows TEM images of cubic nanocrystals with various sizes. They have a quasi-cubic shape regardless of size. As can be seen in the SAED pattern of Figure 3b, pure cubic symmetry was clearly identified for the CoO nanocrystals. This is also consistent with the XRD data given in spectra d–f of Figure 1. Size control of cubic CoO nanocrystals was also achieved by variations in the precursor concentration and the reaction temperature.

It is noteworthy that both CoO nanocrystals are almost mono-dispersed without additional size- and shape-selection process. Although the reduction mechanism leading from  $\text{Co}(\text{III})(\text{acac})_3$  to  $\text{Co}(\text{II})\text{O}^5$  and the source of oxygen have not been clearly determined, oleylamine may act as the reductant and the CoO oxygen may originate from the acac ligand. Several metal oxides have been previously prepared by thermal decomposition of metal acetylacetonate complexes under an inert atmosphere.<sup>2a–c,7</sup>

It has been reported that phases of metal oxide nanocrystals can be tuned by adding an external reagent in the reaction system<sup>8</sup> or by pressure-driven transformation.<sup>9</sup> The successful isolation of both hexagonal and cubic CoO phases in our studies, however, seems to be associated with formation of the kinetic and thermodynamic precursors leading to seeds of two different phases at higher temperatures. The green precursor believed to be  $\text{Co}(\text{acac})_3$  may produce hexagonal seeds upon abrupt heating to 200 °C. On the other hand, the red precursor, presumably an oleylamine-substituted cobalt complex formed by prolonged heating at 135 °C, provides cubic seeds. Most cobalt amine complexes are known to have red color.<sup>10</sup> It is worth mentioning that intermediate reaction times between 30 min and 3 h at 135 °C lead to mixtures of both hexagonal and cubic CoO nanocrystals.

The temperature-dependent magnetic properties of the hexagonal and cubic CoO nanocrystals, measured in both field-cooled and zero-field-cooled conditions by using SQUID were very sensitive to the structural phase but appeared to be irrelevant to the size.<sup>5</sup> All the hexagonal samples showed paramagnetic behaviors, while cubic CoO was antiferromagnetic. The most likely cause of their different magnetic properties is that they have different structural environments surrounding the magnetic Co ions. The cubic rock-salt structure exhibits the 180° Co–O–Co superexchange interactions, in which antiferromagnetic coupling is favored.<sup>11</sup> However, in the hexagonal phase, the exchange interaction between the Co ions through oxygen is not effectively operative due to the tilted Co–O–Co angle (ca. 110°), resulting in the absence of magnetic ordering.

In conclusion, we have prepared previously unknown hexagonal CoO nanocrystals by kinetically tuned thermal decomposition of a single molecular precursor  $\text{Co}(\text{acac})_3$  in oleylamine. The shape and size of CoO nanocrystals are well controlled by changing the precursor concentration and the reaction temperature. A remarkable finding is that phase control between the hexagonal and cubic nanocrystals can be achieved by simple manipulation of the precursor formation kinetics. The successful growth of hexagonal CoO nanocrystals may help to understand the Co-doped ZnO system known as a diluted magnetic semiconductor. We are currently investigating the full mechanistic studies on the preparation and new physical properties for the hexagonal CoO nanocrystals.

**Acknowledgment.** This research at KAIST was supported by the NRL Program of the MOST of Korea. N.H.H. thanks the Creative Research Initiative Program for support of this work. We thank the staffs of KBSI and KAIST for TEM analyses.

**Supporting Information Available:** Synthetic procedures and EELS spectra of CoO nanocrystals, tilted TEM and HRTEM images of hexagonal pyramid-shaped CoO nanocrystals, and ZFC/FC magnetization curves of CoO nanocrystals. This material is available free of charge via the Internet at <http://pubs.acs.org>

## References

- (1) (a) Zeng, H.; Li, J.; Liu, J. P.; Wang, Z. L.; Sun, S. *Nature* **2002**, *420*, 395–398. (b) Tarascon, J.-M.; Armand, M. *Nature* **2001**, *414*, 359–367. (c) Raj, K.; Moskowitz, R. *J. Magn. Magn. Mater.* **1990**, *85*, 233–245.
- (2) (a) Seo, W. S.; Jo, H. H.; Lee, K.; Park, J. T. *Adv. Mater.* **2003**, *15*, 795–797. (b) Seo, W. S.; Jo, H. H.; Lee, K.; Kim, B.; Oh, S. J.; Park, J. T. *Angew. Chem., Int. Ed.* **2004**, *43*, 1115–1117. (c) Sun, S.; Zeng, H.; Robinson, D. B.; Raoux, S.; Rice, P. M.; Wang, S. X.; Li, G. J. *Am. Chem. Soc.* **2004**, *126*, 273–279. (d) Rockenberger, J.; Scher, E. C.; Alivisatos, A. P. *J. Am. Chem. Soc.* **1999**, *121*, 11595–11596. (e) Hyeon, T. *Chem. Commun.* **2003**, 927–934. (f) Jana, N. R.; Chen, Y.; Peng, X. *Chem. Mater.* **2004**, *16*, 3931–3935.
- (3) (a) Skumryev, V.; Stoyanov, S.; Zhang, Y.; Hadjipanayis, G.; Givord, D.; Nogués, J. *Nature* **2003**, *423*, 850–853. (b) Lin, H.-K.; Chiu, H.-C.; Tsai, H.-C.; Chien, S.-H.; Wang, C.-B. *Catal. Lett.* **2003**, *88*, 169–174. (c) Koshizaki, N.; Yasumoto, K.; Sasaki, T. *Sens. Actuators, B* **2000**, *66*, 122–124.
- (4) (a) Yin, J. S.; Wang, Z. L. *Phys. Rev. Lett.* **1997**, *79*, 2570–2573. (b) Verelst, M.; Ely, T. O.; Amiens, C.; Snoeck, E.; Lecante, P.; Mosset, A.; Respaud, M.; Broto, J. M.; Chaudret, B. *Chem. Mater.* **1999**, *11*, 2702–2708. (c) Zhang, L.; Xue, D.; Gao, C. *J. Magn. Magn. Mater.* **2003**, *267*, 111–114. (d) Xu, C.; Liu, Y.; Xu, G.; Wang, G. *Chem. Phys. Lett.* **2002**, *366*, 567–571.
- (5) See Supporting Information.
- (6) (a) Cheng, B.; Samulski, E. T. *Chem. Commun.* **2004**, 986–987. (b) Pacholski, C.; Kornowski, A.; Weller, H. *Angew. Chem., Int. Ed.* **2002**, *41*, 1188–1191.
- (7) (a) Nasibulin, A. G.; Altman, I. S.; Kauppinen, E. I. *Chem. Phys. Lett.* **2003**, *367*, 771–777. (b) Ryabova, L. A.; Salun, V. S.; Serbinov, I. A. *Thin Solid Films* **1982**, *92*, 327–332.
- (8) Wang, X.; Li, Y. *J. Am. Chem. Soc.* **2002**, *124*, 2880–2881.
- (9) Morgan, B. J.; Madden, P. A. *Nano Lett.* **2004**, *4*, 1581–1585.
- (10) Weast, R. C. *CRC Handbook of Chemistry and Physics*; CRC Press: Boca Raton, FL, 1986–1987; pp B87–B88.
- (11) Goodenough, J. B. *Magnetism and the Chemical Bond*; Wiley & Sons: New York, 1963; pp 157–221.

JA050359T